CIDEP of Micellized Radical Pairs in Low Magnetic Fields

Elena Bagryanskaya,*,† Matvey Fedin,† and Malcolm D. E. Forbes‡

International Tomography Center, Siberian Branch, Russian Academy of Sciences, Novosibirsk 630090, Russia, and Venable and Kenan Laboratories, Department of Chemistry, CB#3290, University of North Carolina Chapel Hill, North Carolina 27599

Received: January 28, 2005; In Final Form: March 25, 2005

We report the first experimental study of chemically induced electron spin polarization (CIDEP) processes in low magnetic fields for spin-correlated radical pairs (SCRPs) in micellar environments. Photoexcitation of (2,4,6-trimethylbenzoyl) diphenylphosphine oxide (TMBDPO) leads to the radical pair comprised of acyl radical **1** and phosphonyl radical **2**. The spin polarization, which is very strong in free solution even at zero field, was detected using L-band time-resolved electron paramagnetic resonance (TREPR) spectroscopy with specially modified resonators. The mechanism of formation and decay of low field CIDEP in SCRPs is presented and discussed. The prominent difference between low and high field spectra in micelles is the absence of anti-phase structure for radical **2** with HFI $a > B_0$. This feature is consistent with the proposed polarization mechanism and theoretical predictions.

Introduction

Recently many experimental and theoretical works have been concerned with the radical reactions in low and zero magnetic fields, due to both fundamental interest and possible biological applications.[1,2] Nonequilibrium populations of radical spin levels and their relaxation are among the factors determining the magnitudes of low magnetic field effects. The studies on chemically induced dynamic electron spin polarization (CIDEP) using time-resolved EPR (TREPR) provide for the direct information on these values.

CIDEP phenomena in high magnetic fields are well understood.[3−7] At the present time, several mechanisms of CIDEP formation have been established in observations of noninteracting radicals from both thermal and photochemical reactions. These are the triplet mechanism (TM),[8,9] the radical pair mechanism (RPM),[10−12] the radical-triplet pair mechanism (RTPM),[13−15] and electron spin polarization transfer (ESPT).[4,16] The TM occurs in reactions involving photoexcited triplet states. It arises because of molecular frame anisotropy in the intersystem crossing process (S_1 to T_1) in the excited precursor. This polarization is then transferred to the radicals resulting from, for example, bond cleavage or electron-transfer reactions. A thorough investigation of the TM at different magnetic fields was reported recently.[17] The RPM originates from the interplay of the exchange, electron Zeeman and hyperfine interactions in free radicals undergoing multiple diffusive encounters in free solution. In high magnetic fields where $B_0 \gg a$, (a is the hyperfine interaction (HFI) constant), the electron spin polarization is mainly formed due to $S-T_0$ transitions in the radical pair (ST_0 RPM). If the magnetic field and the HFI constant are comparable ($B_0 \sim a$), the ST_- and ST_+ electron−nuclear transitions can contribute to the formation of additional polarization ($ST_\pm$RPM).

For the radical pairs with relatively long lifetime, e.g., RPs in micelles or in solvents of very high viscosity, CIDEP is formed due to the spin correlated RPM (SC RPM).[18] An interesting feature of the SC RPM is the antiphase splitting (APS) in the EPR spectra of radical pairs, where each individual hyperfine line is split into doublets of opposite phase (emissive/absorptive, E/A, or absorptive/emissive, A/E). Many experimental observations of radical pairs exhibiting APS have been reported, and several theoretical models to describe the spectral shape of the APS have been proposed.[18−24] Closs, Forbes, and Norris[18] were the first to explain the resonance shifts in terms of a constant effective exchange interaction. Later,[19,20] this model was modified by taking into account modulation of the exchange interaction caused by the diffusion of the radicals. Neufeld and coauthors[21,22] demonstrated theoretically that the role of the detecting transverse microwave field may be involved in the origin of the APS.

Most of the studies on CIDEP have been carried out at high magnetic fields ($B_0 \gg a$). However, CIDEP essentially depends on magnetic field, and an important information on interactions in RPs can be obtained studying the magnetic field dependence of the CIDEP.[15,17,25−29] Recently, we have observed and reported on CIDEP in low magnetic field $B_0 < a$ in homogeneous solutions.[25−27] This low field electron−nuclear polarization (ENP) was found to significantly exceed the high field CIDEP in intensity. We also found that the TREPR spectra are asymmetric, with the predominate intensity of the low field spectral line(s). Our theoretical analysis showed that the intensity of the polarization should increase with the viscosity of the solvent. For this reason, one would expect a further increase in polarization formed in micellized RPs. On the other hand, paramagnetic relaxation in the RP is expected to be more efficient in micelles compared to homogeneous solution.

In this paper, we continue our study of low field CIDEP phenomena and apply the technique and theory to micellized RPs consisting of radicals **1** and **2** illustrated in Scheme 1. Specifically, radical pairs were created by 308 nm excimer laser flash photolysis of (2,4,6-trimethylbenzoyl) diphenylphosphine oxide (TMBDPO), in aqueous surfactant solutions containing sodium dodecyl sulfate (SDS) or sodium octyl sulfate (SOS).

* Corresponding author. E-mail: elena@tomo.nsc.ru.
† Russian Academy of Sciences.
‡ University of North Carolina Chapel Hill.

10.1021/jp050499p CCC: $30.25
Published on Web 05/19/2005

SCHEME 1

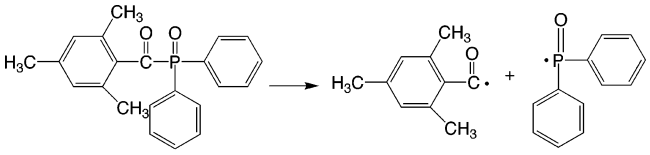

TMBDPO **1** **2**

TMBDPO undergoes α-cleavage upon irradiation from the excited triplet state and forms triplet radical pairs of acyl radicals (**1**) and phosphonyl radicals (**2**).[30] Radical **2** [$(Ph)_2(O)P^{\bullet}$] possesses a large HFI constant $a(^{31}P) \approx 36.5$ mT in addition to a small hyperfine coupling (~0.1 mT) due to the protons on the phenyl groups.[31] It is the large value of the HFI constant of the ^{31}P nucleus that allows us to use L-band TREPR with a resonance frequency in the 1−2 GHz region for investigating the transitions in very low and zero magnetic fields.

We are interested in the effect of confinement of the RP on the generation and CIDEP decay kinetics due to SC RPM and on the spectral shape of the APS in such conditions. Below, our L-band TREPR results are compared to results for the same radicals in homogeneous solution[26] and to the those obtained for RPs in micelles at high magnetic fields.[20]

Low Field CIDEP in Micellized RPs: Qualitative Predictions from Theory

The major differences between low and high field CIDEP can be understood qualitatively by considering the energy level structure at low field. The spin Hamiltonian of the RP (radicals A and B), where only radical A has a single magnetic nucleus, can be written as follows:

$$\hat{H}(r) = \omega_A \hat{S}_{Az} + a\hat{S}_A\hat{I}_A + \omega_B \hat{S}_{Bz} - J(r)(1/2 + 2\hat{S}_A\hat{S}_B) \quad (1)$$

where ω_A and ω_B are the electron Larmor frequencies of radicals A and B respectively, a is the isotropic HFI constant, $J(r)$ is the exchange interaction, and spin operators $\hat{S}$ and $\hat{I}$ have their usual meanings. The effects of HFI anisotropy on CIDEP formation in liquids are usually neglected due to the averaging by rapid radical rotations. This assumption is also upheld for RPs in micelles, since the rotations of radicals (~200−600 ps[32]) are still too rapid comparing to the characteristic times of the CIDEP formation. The nuclear Zeeman interaction was neglected, and $\omega_A = \omega_B = \omega_e$ assumed for brevity. The dependence of the exchange interaction on the inter-radical distance r has the form

$$J(r) = J_0 \exp(-(r - R)/\lambda) \quad (2)$$

where J_0 is the exchange interaction at the radius of closest radical approach R, and λ is a parameter characterizing the exponential decay of the exchange interaction.

At the distance of closest approach of the radicals, where $|J| \gg |a|$, B_0, the eigenfunctions of the RP are described by eq 3

$$S|\alpha_n\rangle, S|\beta_n\rangle, T_+|\alpha_n\rangle, T_+|\beta_n\rangle, T_0|\alpha_n\rangle, T_0|\beta_n\rangle, T_-|\alpha_n\rangle, T_-|\beta_n\rangle \quad (3)$$

where S, T_0, T_+, and T_- are the singlet and triplet functions of the electrons, and the subscript n represents the nuclear spin 1/2 in radical A.

At large distances r, where $|J| \ll |a|$, B_0, the eigenfunctions of the RP are represented by the direct products of the eigenfunctions of the individual radicals. The eigenfunctions of radical B are $|\alpha_B\rangle$ and $|\beta_B\rangle$. The eigenfunctions of radical A in low magnetic field are given by Breit and Rabi[33]

$$|1\rangle = |\alpha_A\alpha_n\rangle$$
$$|2\rangle = C_1|\alpha_A\beta_n\rangle + C_2|\beta_A\alpha_n\rangle$$
$$|3\rangle = |\beta_A\beta_n\rangle$$
$$|4\rangle = C_2|\alpha_A\beta_n\rangle - C_1|\beta_A\alpha_n\rangle \quad (4)$$

where

$$C_1^2 = \frac{1}{2}\left(1 + \frac{\omega_e}{\sqrt{\omega_e^2 + a^2}}\right), \quad C_2^2 = \frac{1}{2}\left(1 - \frac{\omega_e}{\sqrt{\omega_e^2 + a^2}}\right)$$

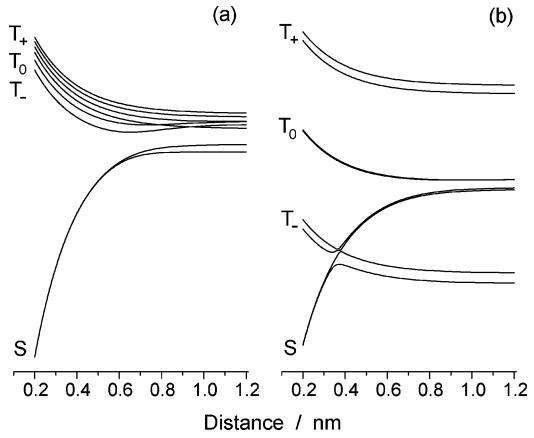

Figure 1. Theoretical scheme for the energy levels of a RP with one magnetic nucleus as a function of interradical distance: $J(r) = J_0 \exp(-(r - R)/\lambda)$ $J_0 = 400$ mT, $R = 0.2$ nm, $\lambda = 0.2$ nm, $a = 36.5$ mT, and $B_0 = 20$ mT (a) and 350 mT (b).

Figure 1a shows the energy levels of the RP at low magnetic field $B_0 < a$ as a function of interradical distance. The diffusive separation of the radicals is adiabatic if $\tau_v \gg a^{-1}$, where τ_v is the correlation time of the velocity of relative motion of the RP.[34] The separation is nonadiabatic if $\lambda^2/D \ll a^{-1}$, where D is the mutual diffusion coefficient. If the separation of the radicals is adiabatic, the populations of the spin levels at $|J| \ll |a|$ are directly correlated with the populations of the corresponding levels at $|J| \gg |a|$. If the separation of radicals is nonadiabatic, the populations of spin levels immediately after separation can be calculated projecting the spin states of the RP at $|J| \gg |a|$ onto the spin states of the individual (separated) radicals at $|J| \ll |a|$. In nonviscous solutions the criterion of nonadiabaticity is usually fulfilled. In viscous solutions such as micelles, a contribution from adiabaticity cannot be neglected for radicals with large HFI, which are used in this work.

It was shown recently that the efficiency of TM for phosphonyl radicals is optimized at the X-band magnetic fields.[17] The contribution of the TM decreases going to both higher and lower magnetic fields. Nevertheless, it is important to examine which polarization patterns can in principle be observed due to TM at low magnetic fields, i.e., how the populations of spin states at $|J| \gg a$ are transferred to the populations of low-field eigenstates at $|J| \ll a$.

For the case of nonadiabatic radical separation at low magnetic fields, the calculations show that for any initial populations at $|J| \gg a$ all CIDEP lines should have the same phase, similarly to the high magnetic field. However, the low-field CIDEP spectra have an asymmetric shape. For example, if only the states $T_-|\alpha_n\rangle$ and $T_-|\beta_n\rangle$ have the initial population n_0, the intensities of EPR lines are found

$$I_{A,|1\rangle\leftrightarrow|4\rangle} \propto n_{A,4} - n_{A,1} = C_1^2 n_0/2$$
$$I_{A,|2\rangle\leftrightarrow|3\rangle} \propto n_{A,3} - n_{A,2} = (1 - C_2^2)n_0/2 = C_1^2 n_0/2$$
$$I_{B,|\alpha\rangle\leftrightarrow|\beta\rangle} \propto n_{B,\beta} - n_{B,\alpha} = n_0 \quad (5)$$

where $I_{A,|1\rangle\leftrightarrow|4\rangle}$ and $I_{A,|2\rangle\leftrightarrow|3\rangle}$ are the intensities of the low- and high-field EPR lines of radical A, respectively, and $I_{B,|\alpha\rangle\leftrightarrow|\beta\rangle}$ is the intensity of the line of radical B. Despite the fact that the intensities of both transitions in radical A coincide, one should keep in mind that as a rule these transitions are detected experimentally at different magnetic fields, and therefore, the experimental TREPR spectrum have an asymmetric shape at low fields.

For a RP with initially populated T_+ states, the EPR lines will be emissive and the intensities described again by eq 5. When only the T_0 state is populated, no TREPR signal is observed. Therefore, for arbitrary initial populations of the triplet levels of the RP, all lines in the spectrum should have the same phase, but the low field line of radical A should be less intense than the high field one.

The case of adiabatic separation can be considered in a manner similar to ref 24. The six upper spin levels at $|J| \gg |a|$ are adiabatically correlated with the six upper levels at $|J| \ll |a|$. After the separation, the two lower levels of the RP (Figure 1a) will not be populated, whereas the six upper levels will be populated. Therefore, the low field TREPR resonance line of radical A can only be emissive, while the high field line can be emissive or absorptive depending on the anisotropy of the intersystem crossing process in the triplet precursor molecule. Consequently, the contribution from the adiabatic process results in specific characteristics of the TREPR spectra due to the TM.

We have shown previously[25,26] that the RPM polarization patterns are similar in both cases of adiabatic and nonadiabatic separation of radicals at low magnetic field. In the nonadiabatic case, the following expressions for the populations of the spin levels of radical A were obtained for $B_0 = 0$

$$n^0_{A,1} = n^0_{A,2} = n^0_{A,3} = \frac{1}{4} + \frac{\sqrt{a\tau_j}}{48\sqrt{2}}\left(\pi + \frac{R}{\lambda} + \ln\left|J_0\tau_j\right| + 2\gamma\right)$$
$$n^0_{A,4} = \frac{1}{4} - \frac{\sqrt{a\tau_j}}{16\sqrt{2}}\left(\pi + \frac{R}{\lambda} + \ln\left|J_0\tau_j\right| + 2\gamma\right) \quad (6)$$

and for the limiting case of high ($B_0 \gg a$) magnetic field

$$n^\infty_{A,1} = n^\infty_{A,3} = \frac{1}{4} + \frac{\pi\sqrt{a\tau_j}}{48}, \quad n^\infty_{A,2} = n^\infty_{A,4} = \frac{1}{4} - \frac{\pi\sqrt{a\tau_j}}{48} \quad (7)$$

where $\tau_j = \lambda^2/D$, $\gamma \cong 0.577$ is the Euler constant, $aJ < 0$ and it is assumed that $a\tau_j \ll 1$. The radical B is not polarized and net polarization is neglected for this case.

The geminate RPs escape from micelles relatively slowly, much slower than the same RPs escape from their geminate state in ordinary solvents such as benzene. Moreover, the RPs in micelles undergo multiple repetitive encounters with each other, during their lifetime in the micelle, compared with the electron spin relaxation times. Taken together these two processes (re-encounter and relaxation) make the calculation of the spin level populations for micellized RPs very cumbersome. Fortunately, there are two limiting cases defined by a relation between the frequency of encounters (Z) and the magnitude of the HFI. In the case when $|a| \ll$ Z, the evolution of the populations and the populations themselves can be considered in terms of an average Hamiltonian characterized by time-independent parameters. In the case when $|a| \gg$ Z, the RPs can be treated similarly to those in homogeneous solution, because of their rapid loss of spin coherence. In the latter case, any micellar effects will be manifest themselves only as a scaling parameter. For the RPs studied here, the condition $|a| \gg$ Z is fulfilled. Based on the analysis above, it is justifiable to use eqs 6 and 7 in our analysis of micellized RPs for qualitative predictions.

An interesting feature of the system described in Figure 1a is the absence of crossing between the $S|\beta_n\rangle$ and $T_-|\alpha_n\rangle$ electron−nuclear spin states. This surely does not mean that the S−T$_-$ transitions do not occur. The interplay between the flip-flop electron−nuclear spin transitions and exchange relaxation still results in CIDEP, but the process cannot be considered in terms of theories developed for the case when the crossing does take place.

Earlier, we used the energy level diagram shown in Figure 1b for the classification of transitions which participate in the formation of APS in high magnetic fields.[18,20] This scheme qualitatively explains the origin of APS, assuming that the exchange interaction leads to a splitting of each transition in radical A into a doublet with the two components opposite in phase as described above. Equation 6 shows that in zero magnetic field, the three upper levels of radical A are equally populated, whereas the lower level is underpopulated. For reactions in micelles, this means that the 6 upper levels of the SCRP are equally overpopulated, and the two lower levels are equally underpopulated. The same result holds for SCRPs in low magnetic field, except that the populations of the upper spin levels will no longer be equal.[26] Thus, for the $|1\rangle \leftrightarrow |4\rangle$ EPR transition in radical A, both components of the doublet can only have the same phase (emission). A similar prediction is made for the $|2\rangle \leftrightarrow |3\rangle$ transition, where both components of the doublet will be in absorption. This leads to the unambiguous conclusion that for radical A, the APS cannot be observed in low and zero magnetic fields. As we will see below, this conclusion agrees well with the experimental observations.

Experimental Section

All materials and solvents were obtained from Aldrich and used as received. The concentrations used were as follows: TMBDPO − 3 mM, SDS − 0.2 M, and SOS − 0.1 M. The apparatus, including a description of the home-built resonators, is described in detail elsewhere.[25,26]

Results and Discussion

The main features of low field CIDEP of radicals **1** and **2** in nonviscous homogeneous solution have been detailed in ref 26. Micellized RPs exist in a liquid phase of higher viscosity and their mobility is restricted by the micellar boundary. To examine how these two factors manifest themselves in terms of CIDEP mechanisms, we initially investigated the low field CIDEP of these radicals in homogeneous solutions of different viscosities.

Figure 2, panels a−c and d−e, shows L-band TREPR spectra obtained after laser flash photolysis of TMBDPO in benzene and poly(ethylene glycol). The center line and the outer doublet are assigned to radicals **1** and **2** from Scheme 1, respectively. At short delay times after the laser flash, the TREPR spectrum exhibits a strong absorptive electron spin polarization due to the TM[22] and a superimposed E/A polarization pattern. The asymmetry of the spectrum (different intensities of the low field and high field lines) has been discussed in detail in ref 26. In that paper, it was shown that at magnetic fields lower than the

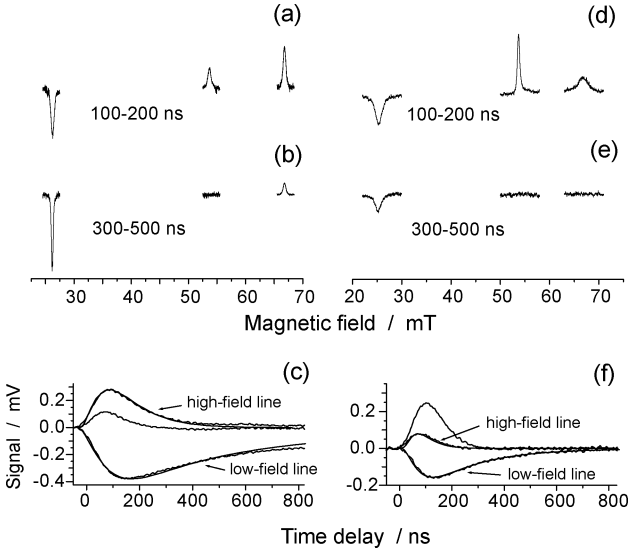

Figure 2. TREPR spectra (a,b) and kinetic decays (c) measured in benzene, and TREPR spectra (d,e) and kinetic decays (f) measured in poly(ethylene glycol) at L-band (1.5 GHz) for radicals **1** and **2** (see Scheme 1 for structures). Numbers shown in figures (a,b,d) and (f) refer to the time delays of the boxcar integration window. The TREPR kinetics of radical **2** are marked by arrows, and the kinetics of radical **1** are not marked.

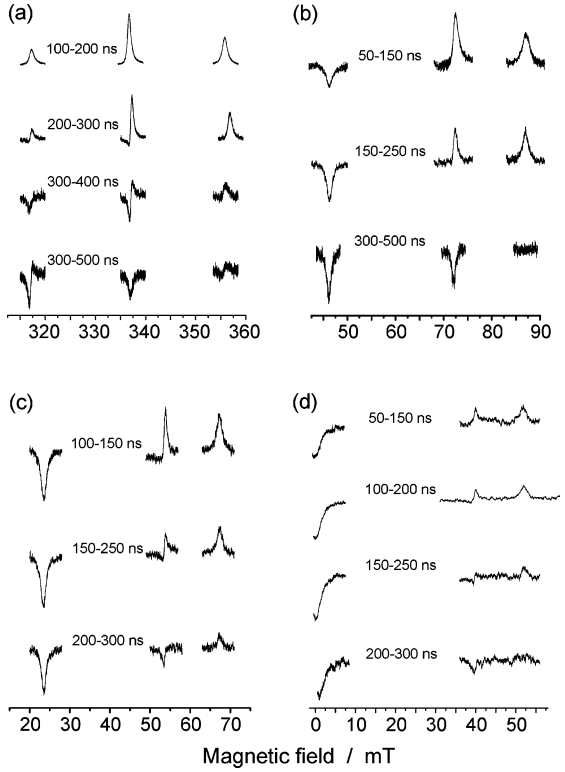

Figure 3. TREPR spectra measured at X-band (a), and L-band: 2 GHz (b), 1.5 GHz (c) and 1 GHz (d). Numbers shown refer to the delay time of the boxcar integration window.

HFI constant, very strong emissive polarization is formed in the low field line. This mechanism is related to the mixing of electron and nuclear spin states of the radical due to $S-T_{\pm}$ transitions at low magnetic field. The main relaxation mechanism for radical **2** is the modulation of the anisotropic HFI.[26] The HFI-induced relaxation rate for the low field line is much slower than for the high field line.[29] This explains the difference in the TREPR kinetics measured for the high and low field lines shown in Figure 2. The anisotropic HFI-induced relaxation is more efficient in viscous solutions, and this is why in poly(ethylene glycol), the decays of both the high and low field lines of radical **2** are faster and the line widths are larger in this solvent.

Analysis of the decay kinetics using the monoexponential function $\exp(-t/\tau_{dec})$ gives (155 ± 5) ns and (490 ± 10) ns for the decay of the high and low field lines, respectively, in benzene. In poly(ethylene glycol) we obtained time constants of (100 ± 5) ns for the high field line and (215 ± 5) ns for the low field line. For more accurate analysis, we used the same simulation approach as in refs 29, 25, and 26, which is based on a numerical solution of the stochastic Liouville equation. In this regard, both kinetic decay traces in benzene can be simulated using the known HFI anisotropy $[A:A] = 228$ mT^2 for this radical[31] and a reasonable correlation time for the rotational motion of radical $\tau_c = 12$ ps (e.g., in ref 26 $\tau_c = 10$ ps was obtained in acetonitrile). The satisfactory fit of the kinetic decay traces of both lines in poly(ethylene glycol) can be obtained using the same HFI anisotropy and value for τ_c of 26 ps. The low field kinetics are also influenced by a second-order chemical reaction, which is included in the simulation using the parameter $2k_tR_0 = 6 \times 10^6$ s^{-1}. Here k_t is the reaction rate constant and R_0 is the initial concentration of the radicals.

Radical **1** experiences CIDEP due to the TM. The experimental conditions were identical in both solvents, and the intensity of this line was much higher in the more viscous poly(ethylene glycol). The decay of the polarization and the line width are approximately the same in both solvents. The TREPR kinetics in both solvents is approximated well using a monoexponential function at $t > 100$ ns with the characteristic decay time $\tau_{dec} = (75 \pm 5)$ ns and thus is determined by relaxation. The value we obtained for τ_{dec} agrees with the results reported previously,[35] where $T_1 < 100$ ns in benzene was estimated at X-band. The TREPR kinetic decay times are very similar in benzene and poly(ethylene glycol), because the spin relaxation of radical **1** is mainly determined by the modulation of the spin-rotational interaction due to the rotation of CO group around C−CO bond.[35] Thus, the increase in polarization of radical **1** in poly(ethylene glycol), in comparison with benzene, is due to an increase in the TM polarization in the higher viscosity solvent. Electron spin relaxation does not play a significant role. We therefore expect stronger polarization due to the TM for radical **1** in micelles compared to nonviscous liquid solutions.

Figure 3 shows X- and L-band TREPR spectra of radicals **1** and **2** obtained in SDS micelles. In high magnetic field (X-band, 9.5 GHz), the contribution of the TM is strong and manifests itself as lines of the same absorptive phase at short delay times for all transitions. At longer delay times, spectral features due to $S-T_-$ and $S-T_+$ CIDEP processes are observed, in addition to APS line shapes. The presence of APS unambiguously proves that SCRPs are observed in micelles, and that any contribution from escaped radicals is negligible on this time scale. The spectra shown in Figure 3a agree well with those from ref 20.

At L-band, (~2 GHz), EPR lines of radical **2** show an E/A pattern even at short delay times. This can be explained by both a decrease of the TM and by an increase of polarization due to $S-T_-$ and $S-T_+$ transitions in the radical pairs. The efficiency of the TM for precursors leading to phosphonyl radicals is optimized at X-band and decreases in both higher and lower magnetic fields.[17] On the other hand, our studies on low field CIDEP of phosphonyl radicals in homogeneous solutions show that the polarization intensity due to $S-T_-$ and $S-T_+$ transitions

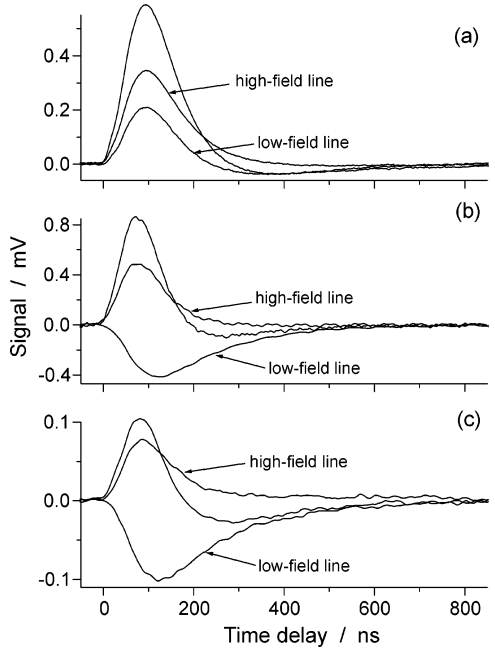

Figure 4. TREPR kinetics of radical **2** (marked by arrows) and radical **1** (not marked) measured at X-band (a) and L-band: 2 GHz (b) and 1.5 GHz (c).

strongly increases in fields comparable to and lower than the HFI constants of the reacting radicals.[26] Both factors lead to the predominance of the E/A pattern for radical **2**.

In contrast to our observations for radical **2**, the polarization of radical **1** in micelles is quite different from that observed in homogeneous solution. The signal is dominated by the TM at early delay times, then contributed to by $S-T_-$ and $S-T_+$ transitions, and finally leading to APS and an inversion of the polarization phase at longer delay times. At even lower magnetic fields (L-band, 1.5 and 1 GHz), a further increase of the low field line intensity is observed, in comparison with the high field line of radical **2** (Figures 3c,d). This is again consistent with the dominant polarization being formed due to $S-T_-$ and $S-T_+$ transitions over the TM at low magnetic fields. We note that APS is detected in radical **2** only at X-band and not at L-band. This observation agrees well with our theoretical considerations above.

Figure 4 shows the TREPR kinetics measured at X-band (9.5 GHz, Figure 4a) and L-band (2 GHz, Figure 4b and 1.5 GHz, Figure 4c). All of the kinetics decay on the time scale of a few hundred ns. The lifetime of the RP in SDS micelles of about 139 ns has been measured previously at zero magnetic field in laser-flash photolysis study of TMBDPO,[36] and using Stimulated Nuclear Polarization at 68 mT it was found to be 151 ns.[37]

The polarization of the radical **1** consists of initially net absorptive polarization due to TM, APS and negative net polarization due to $S-T_-$ transitions generated during the lifetime of the RP. As mentioned above, the main relaxation mechanism for this radical is modulation of the spin-rotational interaction. The TREPR kinetics of radical **1** are very similar at X- and L-bands, and the decay is on the order of 100 ns.

The decay of the high field line of radical **2** is nearly the same at all magnetic fields. A monoexponential fit using $t >$ 100ns gives the values $\tau_{dec} = 70 \div 95$ ns. This value is very close to the electron spin relaxation rate in poly(ethylene glycol). The decay of the low field line slows down significantly at low magnetic fields. The value of τ_{dec} obtained using a monoexponential fit with $t > 150$ ns increasing from (70 ± 5) ns at X-band to (190 ± 5) ns at L-band (1.5 GHz). This increase is determined

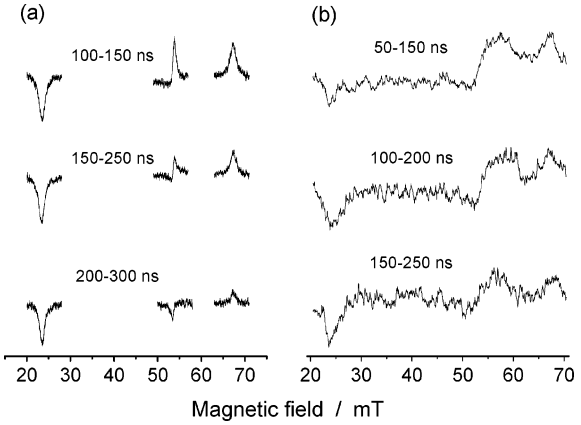

Figure 5. Comparison of TREPR spectra measured at L-band (1.5 GHz) in SDS (a) and SOS (b) micelles. Numbers shown refer to the time delays of the boxcar integration window.

by the magnetic field dependence of the anisotropic HFI-induced relaxation, similar to that in homogeneous solutions as was discussed above. This increases the polarization intensity from $S-T_-$ transitions.

Figure 5 compares low field TREPR spectra measured in SDS vs SOS micelles. Tarasov and co-workers have shown that the APS observed on the same RPs at X-band is significantly more pronounced in SOS micelles comparing to SDS micelles.[20] In this work, however, L-band TREPR spectra of radical **2** do not contain APS in either SDS or SOS micelles. This again confirms the absence of APS at low magnetic field for radical with HFI constants $a > B_0$. At the same time the APS is very well pronounced in radical **1** for both surfactants.

The intensity of the TREPR signal in smaller (SOS) micelles becomes quite poor. This is explained by line broadening due to faster exchange relaxation caused by a faster rate of radical reencounters. Note, that an increase of the line width in SOS micelles is also additional confirmation that the micellized RPs are observed and any contribution from escaped radicals into the bulk is negligible.

Conclusions

In this paper, we have examined the general features of low field CIDEP in micellized SCRPs with one large HFI constant. We have determined that the CIDEP pattern in micelles looks similar to that in homogeneous solutions for radicals with HFI $a > B_0$ but is very different from CIDEP of SCRPs observed at high magnetic field. The major differences in polarization formation manifest themselves as an asymmetric shape of the observed spectra even at very short delay times, and by the absence of any anti-phase structure. The main features of the polarization decay in low magnetic fields are manifested as different kinetics measured for the high and low field TREPR transitions. Polarization of radicals without nonzero HFI constants shows APS and net emission due to the $S-T_-$ mechanism.

Acknowledgment. We thank Dr. V. F. Tarasov and Prof. P. A. Purtov for helpful discussions. This work was supported by the National Science Foundation (Grant # CHE-0213516) and the Russian Foundation for Basic Research (Grant # 04-03-32604).

References and Notes

(1) Ritz, T.; Thalau, P.; Phillips, J. B.; Wiltschko, R.; Wiltschko, W. *Nature* **2004**, *429*, 177 and references therein

(2) Timmel, C. R.; Cintolesi, F.; Brocklehurst, B.; Hore, P. J. *Chem. Phys. Lett.* **2001**, *334*, 387 and references therein
(3) Salikhov, K. M.; Molin, Yu. N.; Sagdeev, R. Z.; Buchachenko, A. L. *Spin Polarization and Magnetic Effects in Radical Reactions*; Molin, Yu. N., Ed; Elsevier: Amsterdam, 1984.
(4) McLauchlan, K. A. In *Modern Pulsed and Continuous-Wave Electron Spin Resonance*; Kevan, L., Bowman, M. K., Eds.; Wiley: New York, 1990; pp 285−363.
(5) Steiner, U. E.; Ulrich, T. *Chem. Rev.* **1989**, *89*, 51.
(6) Nagakura, S.; Hayashi, H.; Azumi, T. *Dynamic Spin Chemistry: Magnetic Controls and Spin Dynamics of Chemical Reactions*; Kodasha Ltd.: Tokyo, 1998.
(7) Van Willigen, H. In: *Molecular and Supramolecular Photochemistry*; Ramamurthy, V., Schanze, K. S., Eds.; Dekker: New York, 2001; Vol. 6, pp 197−247.
(8) Atkins, P. W.; Evans, G. T. *Mol. Phys.* **1974**, *27*, 1633.
(9) Pedersen, J. B.; Freed, J. H. *J. Chem. Phys.* **1975**, *62*, 1706.
(10) Freed, J. H.; Pedersen, J. B. *Adv. Magn. Reson.* **1976**, *8*, 1.
(11) Adrian, F. J. *Chem. Phys. Lett.* **1981**, *80*, 106.
(12) Adrian, F. J.; Monchick, L. *J. Chem. Phys.* **1979**, *71*, 2600.
(13) Blättler, C.; Jent, F.; Paul, H. *Chem. Phys. Lett.* **1990**, *166*, 375.
(14) Shushin, A. I. *J. Chem. Phys.* **1993**, *99*, 8723.
(15) Stavitski, E.; Wagnert, L.; Levanon, H. *J. Phys. Chem. A* **2005**, *109*, 976.
(16) Fujisawa, J. I.; Ishii, K.; Ohba, Y.; Iwaizumi, M.; Yamauchi, S. *J. Phys. Chem.* **1995**, *99*, 17082.
(17) Makarov, T.; Savitsky, A.; Möbius, K.; Beckert, D.; Paul, H. *J. Phys. Chem.* in press.
(18) Closs, G. L.; Forbes, M. D. E.; Norris, J. R. *J. Phys. Chem.* **1987**, *91*, 3592.
(19) Tarasov, V. F.; Yashiro, H.; Maeda, K.; Azumi, T.; Shkrob, I. A. *Chem. Phys.* **1996**, *212*, 353
(20) Tarasov, V. F.; Yashiro, H.; Maeda, K.; Azumi, T.; Shkrob, I. A. *Chem. Phys.* **1998**, *226*, 253.
(21) Neufeld, A. A.; Purtov, P. A.; Doktorov, A. B. *Chem. Phys. Lett.* **1997**, *273*, 311.
(22) Neufeld, A. A.; Pedersen, J. B. *J. Chem. Phys.* **2000**, *113*, 1595.
(23) Shushin, A. I. *Chem. Phys. Lett.* **1991**, *177*, 338.
(24) Salikhov, K. M. *Appl. Magn. Reson.* **1997**, *13*, 415.
(25) Bagryanskaya, E. G.; Yashiro, H.; Fedin, M.; Purtov, P.; Forbes, M. D. E. *J. Phys. Chem. A* **2002**, *106*, 2820.
(26) Fedin, M. V.; Yashiro, H.; Purtov, P. A.; Bagryanskaya, E. G.; Forbes, M. D. E. *Mol. Phys.* **2002**, *100*, 1171.
(27) Bagryanskaya, E.; Yashiro, H.; Fedin, M.; Purtov, P.; Forbes, M. D. E. *Riken Rev. Focused Magn. Field Spin Effects Chem. Relat. Phenom.* **2002**, *44*, 116.
(28) Fedin, M. V.; Purtov, P. A.; Bagryanskaya, E. G. *J. Chem. Phys.* **2003**, *118*, 192.
(29) Fedin, M. V.; Purtov, P. A.; Bagryanskaya, E. G. *Chem. Phys. Lett.* **2001**, *339*, 395.
(30) Kamachi, M.; Kuwata, K.; Sumiyoshi, T.; Schnabel, W. *J. Chem. Perkin Trans. 2* **1988**, 961.
(31) *Landolt-Bornstein, New Series, Group 2*; Fischer, H., Hellwege, K. H., Eds.; Springer: Berlin, 1977; Vol. 9.
(32) Tarasov, V. F.; Ghatlia, N. D.; Avdievich, N. I.; Turro, N. J. *Z. Physik. Chem.* **1993**, *182*, 227.
(33) Breit, G.; Rabi, I. I. *Phys. Rev.* **1931**, *38*, 2081.
(34) Shushin, A. I. *Chem. Phys. Lett.* **1988**, *146*, 297.
(35) Makarov, T. N.; Bagryanskaya, E. G.; Paul, H. *Appl. Magn. Reson.* **2004**, *26*, 1.
(36) Hayashi, H.; Sakaguchi, Y.; Kamachi, M.; Schnabel, W. *J. Phys. Chem.* **1987**, *91*, 3936.
(37) Ananchenko, G. S.; Bagryanskaya, E. G.; Tarasov, V. F.; Sagdeev, R. Z.; Paul, H. *Chem. Phys. Lett.* **1996**, *255*, 267.